Hydrogen atom in a strong magnetic field: Semiclassical quantization using classical adiabatic invariance

Subhash Saini* and David Farrelly
Department of Chemistry and Biochemistry, University of California, Los Angeles, California 90024
(Received 21 April 1987)

The method of adiabatic switching (AS) is applied to the problem of a hydrogen atom in a strong magnetic field, i.e., the quadratic Zeeman effect (QZE). The QZE is one of the simplest realistic physical problems exhibiting classical chaos which presents conceptual and computational obstacles to the implementation of many semiclassical quantization methods, while the highly nonseparable nature of the problem makes exact quantum treatments problematic. The AS method is straightforward, mainly involving integration of Hamilton's equations of motion, and in addition, unlike most other trajectory-based semiclassical methods, works even in mildly chaotic volumes of classical phase space. In AS, a zeroth-order classical torus is quantized and then the perturbation is switched on adiabatically using a time-dependent or time-independent switching function which is incorporated into the Hamiltonian. A central problem in AS is the choice of the most appropriate zeroth-order tori. Based on a comprehensive study of the classical dynamics of the QZE it is shown that the best zeroth-order tori for AS are those obtained by quantizing the zeroth-order Hamiltonian (i.e., the hydrogen atom) and simultaneously an adiabatic invariant found by Solov'ev. AS is performed for a wide variety of magnetic fields and energies including states lying in mildly chaotic regions of phase space where Solov'ev's invariant is no longer conserved. Results are generally in excellent agreement with exact quantum results, and additionally the method is self-diagnostic, yielding large standard deviations in energies should it begin to fail. However, AS is seen to break down in the strongly chaotic regions of phase space where the quantum levels display multiple avoided crossings (strongly n-mixing regime). Application of AS to the QZE leads to a number of new developments in the theory of AS, including AS in extended phase space where the Hamiltonian is explicitly independent of time.

I. INTRODUCTION

The Stark and Zeeman effects in hydrogen are often chosen as the prototypical examples of the behavior of atoms subject to strong electric and magnetic fields.[1] Though the hydrogenic Stark effect is, perhaps, one of the most straightforward realistic problems in atomic physics[1-4] this is by no means the case for the quadratic (diamagnetic) Zeeman effect (QZE). Labeled the "trouble with hydrogen"[5] the QZE remains one of the major unsolved basic problems of atomic physics.[6,7] Despite numerous investigations (including perturbation,[8-16] semiclassical[17,18] and exact quantum calculations[19-29]) it is not yet possible to predict *quantitatively* the evolution of arbitrary energy levels as a function of magnetic field strength from the zero-field limit to the regime where the magnetic and Coulomb fields are comparable,[5] although there has recently been substantial progress made in the development of exact quantum methods.[26-29] Since sufficiently high Rydberg states can always be found for which the coupling of the electron to the Coulomb and the magnetic fields is approximately equal, the QZE is of much relevance to understanding the properties of Rydberg atoms in external fields.[1,5-7,30] The QZE is also important astrophysically where magnetic fields of the order of 10^8 G exist on white dwarf stars and as high as 10^{12} G at the polar caps of neutron stars.[31-34] It is also potentially of great importance in understanding impurity states of semiconductors in external uniform magnetic fields.[35] An excellent review of the Zeeman effect up to 1977 has been given by Garstang,[36] while a number of more specialized reviews have appeared since.[6,7,30,37-40]

A basic difference between the Stark and quadratic Zeeman effects concerns the integrability of the respective Hamiltonians. Under a static electric field the Runge-Lenz vector in modified form is preserved as a constant of motion for the hydrogen atom.[3,4] An important consequence is that the Stark Hamiltonian is separable (in parabolic coordinates) which makes numerical solution of the problem quite straightforward.[4] In contrast, the quadratic Zeeman Hamiltonian is neither separable nor integrable because the external magnetic field destroys the supersymmetry of the purely Coulombic problem.[6] This may be understood by considering two opposite integrable limits of the Hamiltonian: in the limit of zero applied field the problem exhibits *spherical* symmetry while in the opposite Landau limit where the magnetic field dominates, *cylindrical* symmetry is observed. In the Landau region the problem approximates a free electron in a uniform magnetic field and the energy spectrum consists of a series of equally spaced lines.[6] The situation is much more complicated in the "mixing" region where the Coulombic and magnetic forces are comparable and both of the limiting symmetries are effectively destroyed. Although this might give rise to

the expectation of a complicated, unassignable atomic spectrum, experiments on the QZE in Rydberg atoms reveal spectra which display remarkable regularities, termed quasi-Landau resonances, near and above threshold.[41–44] A major success of classical[44,45] or approximate one dimensional semiclassical[46–51] methods is the prediction of the $1.5\hbar\omega$ quasi-Landau resonance *spacings* observed through threshold, but these theories have been much less useful in estimating *absolute* values of energy eigenvalues. The observation of the quasi-Landau resonances has prompted various experimental studies of the QZE which in turn has led to numerous theoretical attempts to find an approximate symmetry or constant of motion as a way of understanding and interpreting the regularities in the spectrum.[6,18,34,38,52–58] In particular, exact quantum variational calculations of oscillator strengths for dipole transitions to high Rydberg states by Clark and Taylor[22,23] using a Sturmian basis revealed that as a function of energy the oscillator strengths appeared to be a superposition of several apparently independent series, each of which contained almost equally spaced lines. In addition, many near coincidences of energy levels of lines from *different* series were observed, supporting the existence of an approximate dynamical symmetry. Clark and Taylor[52] were also able to relate the "extra constant" to the important phenomenon of motion along a potential ridge described by Fano.[59,60] The strong nonseparability of the QZE and the necessity of including the continuum makes exact quantum calculations difficult or intractable [depending on the state(s) of interest and the magnetic field strength]. On the other hand, quantum perturbation theory is accurate only for small magnetic fields; the perturbation overwhelms the zeroth-order Hamiltonian for magnetic fields of interest in the QZE and the method fails.[12,16] Partly for such computational reasons, much effort has been devoted to classical and semiclassical studies since it is relatively easy to compute the exact classical dynamics over a wide range of energies and magnetic field strengths.[18,34,61–66] It is worth pointing out, however, that even a purely classical study presents a number of interesting technical problems which will be discussed in more detail in Sec. II. Another important reason for classical and semiclassical studies of the QZE concerns the possible relevance of classical chaos to quantum mechanics; the QZE is noteworthy in being the simplest real system in atomic and molecular physics whose classical dynamics is chaotic.[18,34,61–64,66] Although the phenomenon of classical chaos is well characterized in nonintegrable systems, the quantum consequences (if any) of chaos remain undetermined. In pursuit of this question, a large number of classical and semiclassical investigations have been made and a prodigious literature exists which has been reviewed extensively.[67–71] However, the majority of classical and semiclassical studies have been directed towards essentially model problems like the Henon-Heiles Hamiltonian. In addition, the theory of semiclassical quantization of integrable but highly nonseparable systems is itself not completely developed as recent studies of coupled oscillator problems with internal nonlinear resonance have revealed.[72–74] Thus, extensions to genuinely nonintegrable systems are not trivial.

Rydberg atoms in external fields[75–77] provide a unique opportunity to study the issue of semiclassical quantization and chaos as it is possible to compare the predictions of classical and semiclassical methods to both exact quantum calculations and experimental observations for many combinations of principal quantum number and magnetic field strength.[5–7,37–40] The discovery of the quasi-Landau spacings experimentally by Garton and Tomkins[41] has led to numerous experimental studies of the QZE, primarily in alkali-metal atoms using atomic beams and pulsed dye lasers, and lately using cw dye lasers it has been possible to produce and study high Rydberg states of heavy alkali-metal atoms such as cesium.[78,79,45] Very recently, there have been studies of quite high lying states of lithium[80,81] and also direct studies of the QZE in hydrogen itself.[44] Excellent surveys of the experimental situation have been given by Gay[6] and by Delande *et al.*[45]

For the reasons described, the QZE is rapidly becoming a "test bed" for the development of semiclassical quantization schemes[18,62–64,82] and simultaneously for the study of quantum chaos.[29,82,83] There have been several purely classical studies of the QZE which, through examination of classical trajectories and Poincaré surfaces of section, have revealed a strong transition to chaotic motion as either the energy or the magnetic field is increased.[18,34,62–66] When the dynamics is mainly regular the surfaces of section consist of nested curves indicating the existence of classical tori (equivalently, of an approximate constant of motion).[67,68] As the electron begins to feel roughly equal coupling to the magnetic and Coulomb fields the tori start to break down and the surfaces of section no longer consist of closed curves, indicating that the trajectories are not confined to the surfaces of invariant tori. Nonetheless, the existence of tori suggests that semiclassical quantization methods might be feasible, at least in the regular regime, and there have, in fact, been some previous semiclassical studies of the QZE.[18,62–64,82] Using classical trajectories and Poincaré surfaces of section, Delos *et al.*[62,63] quantized low-lying states of the QZE existing exclusively in regular regions of classical phase space, but restricted their calculations to states with $|m|>0$ (m is the magnetic quantum number) possibly to avoid problems associated with the Coulomb singularity in the Hamiltonian which is important when $m=0$. Although the method is extendable (in a nontrivial way, see Sec. II A) to $m=0$ states, a more serious drawback to their way and most other trajectory-based ways of imposing Einstein-Brillouin-Keller[67–70] (EBK) quantization is their failure when the dynamics becomes chaotic. An alternative approach which is most useful for resonance (quasi-Landau) states has been developed by Noid *et al.*[64] who used a classical analog of the Born-Oppenheimer approximation to treat states above the classical ionization threshold where two widely disparate frequencies characterize the problem: the frequency in the field direction and the frequency in the direction transverse to it. For most *bound* states, particularly those in the mixing regime,[6] this kind of

treatment is not possible because there are numerous overlapping nonlinear resonances which precludes a dynamical separation relying on clearly different frequencies. A different type of semiclassical method based on classical perturbation theory overcomes most of the shortcomings of trajectory-based EBK quantization by constructing and quantizing the tori *directly*,[18] i.e., explicit expressions (*divergent* series expansions[69,70]) for approximate constants of motion are obtained. For the QZE Solov'ev[53,54] derived an analytical expression, valid in the weak-field limit, for the approximate classical constant of motion using first-order classical perturbation theory which he proceeded to quantize. The quantum-mechanical operator corresponding to Solov'ev's invariant was obtained independently by Herrick[56] using group theory (see also Refs. 57 and 58). For the special case that $m=0$ Birkhoff-Gustavson normal-form (BGNF) theory has been used[18] to obtain a much-higher-order representation of the approximate constant than obtained by Solov'ev; this approximate constant was used as the basis for quantizing the QZE in both regular *and* chaotic volumes of classical phase space where only remnants of tori exist ("vague" tori[85]).[18] Although good agreement with exact quantum calculations was obtained for some states, it seems likely that a much-higher-order representation of the constant of motion[86] in conjunction with the recently developed Lie algebraic approach to semiclassical quantization[74] might be necessary.

Recently a simple and straightforward approach to the problem of semiclassical quantization has been developed known as adiabatic switching (AS). This approach is computationally and conceptually quite straightforward and, unlike most other trajectory-based methods, works even in mildly chaotic regions of phase space. The AS method was originally developed by Solov'ev[87] for the calculation of vibrational energy eigenvalues in a model coupled-oscillator problem and was subsequently applied by him and Grozdanov[88] to the hydrogen atom in crossed electric and magnetic fields, but note that their calculation was limited to the ground state plus two other very-low-lying states. AS has recently been rediscovered by Johnson[89,90] which has since generated renewed interest in the method, particularly in applications to model molecular Hamiltonians,[91–95] and has also been applied in optics.[96] In AS a suitable zeroth-order reference Hamiltonian is first quantized which serves to specify a zeroth-order classical torus corresponding to a quantum state. The perturbation is then switched on adiabatically as the classical trajectory evolves in time, usually by explicitly incorporating a *time-dependent* switching function into the Hamiltonian [exceptions to the use of a time-dependent Hamiltonian to perform AS are provided by the work of Jaffé[97] and by the present study (see Sec. III C) which differs from Jaffé's method]. If adiabatic invariance holds, preservation of the invariant ensures that the original zeroth-order torus evolves into a quantized, usually much distorted, torus of the full problem. Adiabatic invariance is not exactly preserved for nonintegrable systems, and, because there are no rigorous theorems regarding AS in other than one dimension,[98,99] the method is based largely on empirical studies. Nevertheless, AS appears to work reasonably well provided the dynamics is not too strongly chaotic, and has the additional important advantage of being self-diagnostic (by yielding large standard deviations in energy eigenvalues) should it begin to fail. Note that in the absence of *uniform* semiclassical corrections AS is unable to account for intermanifold avoided crossings of energy levels, which is significant since it has been proposed that chaos might be connected with the occurrence of mutiple avoided crossings of energy levels.[67]

The present study of the QZE represents the first comprehensive application of AS to a realistic physical problem; a wide range of magnetic field strengths are considered for a variety of Rydberg states, including states lying in chaotic volumes of classical phase space. Application of AS to the QZE also leads to a number of new developments in the theory of AS itself, including *time-independent* AS in extended phase space. These developments are discussed in Sec. III.

The paper is organized as follows. In Sec. II the quadratic Zeeman Hamiltonian is introduced and a detailed examination of its classical dynamics made. Also considered in Sec. II is the choice of coordinate system in which to effect quantization. The Coulomb singularity in the Hamiltonian requires that the cases $|m|>0$ and $m=0$ be treated separately. In particular, the $m=0$ QZE Hamiltonian must be regularized and this is described in Sec. II A. An unusual feature of the present application is that in cylindrical coordinates the zeroth-order problem is nonseparable whereas in AS a *separable* zeroth-order reference Hamiltonian is normally used.[87–95] This makes the problem of finding initial conditions on the surface of the zeroth-order torus nontrivial; this is dealt with in Sec. III A. In Sec. III B the time-dependent AS method for states with $|m|>0$ is discussed, and results are presented for several magnetic fields. In Sec. III C the time-independent AS method for $m=0$ states is described together with results of numerical calculations for a range of magnetic field strengths. Time-independent AS is a new development in the theory of AS which may prove useful for perturbed Kepler-like problems and other problems where the Hamiltonian is time dependent (e.g., the hydrogen atom in a microwave field,[100] or atoms and molecules interacting with laser fields). Conclusions are in Sec. IV.

II. CLASSICAL DYNAMICS

Assuming an infinite nuclear mass with the magnetic field directed along the z axis, the classical Hamiltonian for the QZE in cylindrical coordinates and atomic units (i.e., $m_e=e=\hbar=1$), is given by[36]

$$H=\tfrac{1}{2}(P_\rho^2+P_z^2)+V(\rho,z)\ , \tag{2.1}$$

where

$$V(\rho,z)=\frac{P_\phi^2}{2\rho^2}+\frac{1}{8}\gamma^2\rho^2-\frac{Z}{(\rho^2+z^2)^{1/2}} \tag{2.2}$$

and

$$\rho^2=x^2+y^2 ,$$

where $\gamma=B/B_0$ is the reduced uniform magnetic field strength, and $B_0=2.35\times10^5$ T is the field for which the Landau energy equals the Rydberg constant. The paramagnetic contribution to the energy has been removed by transforming to a uniformly rotating frame. A comprehensive description of the construction of the Zeeman Hamiltonian may be found in the review by Garstang.[36] In the limit that $\gamma=0$ the Hamiltonian is simply that of the hydrogen atom while in the opposite limit that the nuclear charge $Z=0$, the Hamiltonian reduces to the Landau problem (i.e., the motion of a charged particle in a uniform magnetic field). Since the angle ϕ does not appear in the Hamiltonian its conjugate momentum P_ϕ is a constant of the motion, and this is the reason the problem can be reduced to two dimensions. P_ϕ corresponds to the z component of angular momentum and is quantized according to the usual prescription,

$$P_\phi=m\hbar \tag{2.3a}$$

with the paramagnetic energy being given by

$$E_p=\gamma(m+2s_z)/2 , \tag{2.3b}$$

where s_z is the spin quantum number.

Classical trajectories obtained by numerically integrating Hamilton's equations of motion for the Hamiltonian (2.1) evolve in a four-dimensional phase space (ρ,P_ρ,z,P_z) according to the potential energy surface given by Eq. (2.2) (see Fig. 1). The Coulomb singularity presents numerical problems when $m=0$ in which case the classical trajectories can penetrate into the nucleus and an infinitely small step size would be required in the integration of the equations of motion. This possibility does not arise when $|m|>0$ because the centrifugal term dominates the Coulombic term close to the origin. Unlike the Stark effect the system is bound for energies less than the classical escape energy ($E_{\rm esc}=\gamma/2|m|$); for energies greater than $E_{\rm esc}$ ionization is possible in the z direction but the motion is bounded in the ρ direction which accounts for the presence of resonances above the ionization energy.[64] Note that the quantum ionization energy is higher than the classical escape energy by the zero-point energy, $\gamma/2$.[34]

Apart from parity, energy is the only exact constant of motion for the Hamiltonian in Eq. (2.1) [P_ϕ appears only as a parameter in Eq. (2.1)] and consequently the Hamiltonian is nonintegrable and the classical trajectories are, in principle, free to explore the entire three-dimensional energy shell. Examination of classical trajectories (Figs. 2 and 3) and Poincaré surfaces of section (Fig. 2) reveals that for low energies and low fields or both, the dynamics is regular and the trajectories are in fact confined to a surface of lower dimensionality than the energy shell. The surfaces of section[18,101] (Fig. 2) suggest that the trajectories evolve on two-dimensional tori embedded in the four-dimensional phase space (each torus is uniquely defined by the particular set of initial conditions used in starting out the trajectory). This points to the existence of an adiabatic invariant in addition to the energy for which Solov'ev has obtained the following expression valid in the weak-field limit using first-order classical perturbation theory[53,54]

$$\Lambda=4A^2-5A_z^2 , \tag{2.4}$$

where $\mathbf{A}$ is the Runge-Lenz vector,[3]

$$\mathbf{A}=\frac{1}{(-2H_0)}\left[\mathbf{L}\times\mathbf{p}-\mathbf{p}\times\mathbf{L})/2+\frac{\mathbf{r}}{r}\right] , \tag{2.5}$$

$\mathbf{L}$ is angular momentum, and

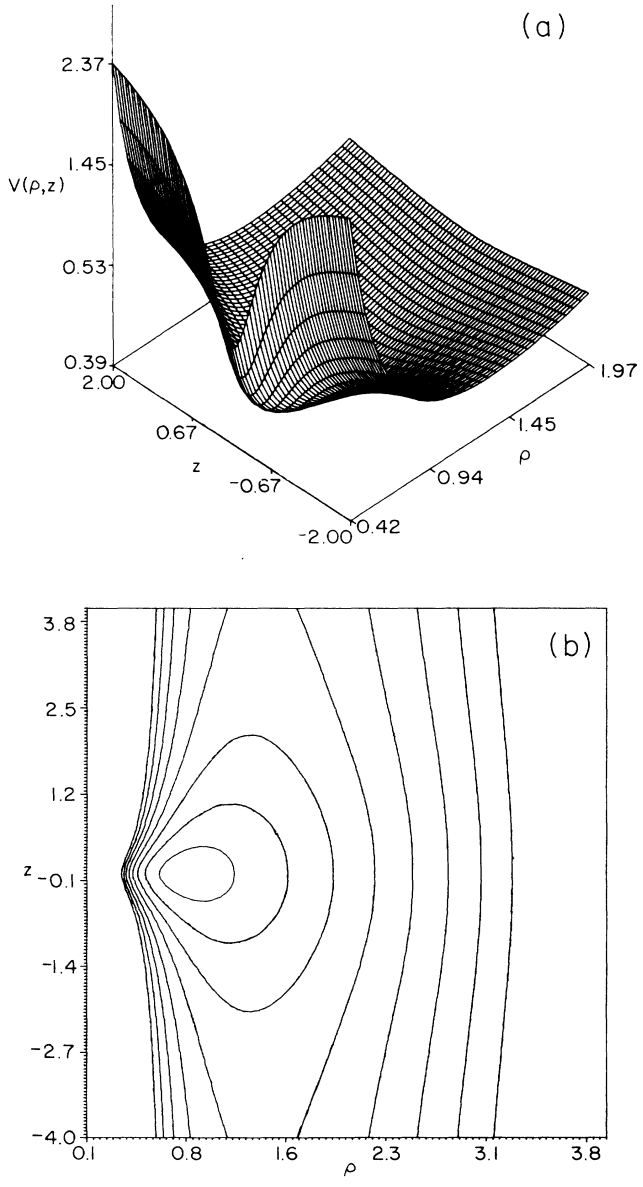

FIG. 1. Isometric and contour plots of the QZE potential Eq. (2.2) in cylindrical coordinates with $m=1$. In (b) the contours are evenly spaced by 0.2 with the lowest contour being -0.3.

$$H_0 = -1/(2n^2), \quad n = 1,2,3,\ldots .$$

When the magnetic field is applied the supersymmetry of the pure Coulomb problem is destroyed and the zero-field periodic motion (closed Kepler ellipses) is distorted into quasiperiodic motion. If the field is turned on sufficiently slowly, Λ is conserved through fourth order in γ. Delande and Gay have summarized the conditions under which Λ is expected to be an invariant in the inequality,[6]

$$\gamma n^3 \ll 1 . \tag{2.6}$$

Evidence that Λ is an approximate constant of motion has also been provided by Hasegawa *et al.*,[102] who compared calculated surfaces of section for $m=0$ trajectories with level curves of the adiabatic invariant Λ, obtaining excellent agreement in the quasiperiodic regime (see also Ref. 18). An alternative *quantum* derivation of Λ by Herrick[56] exploited the separability of the problem within given n manifolds on the Fock hypersphere (this

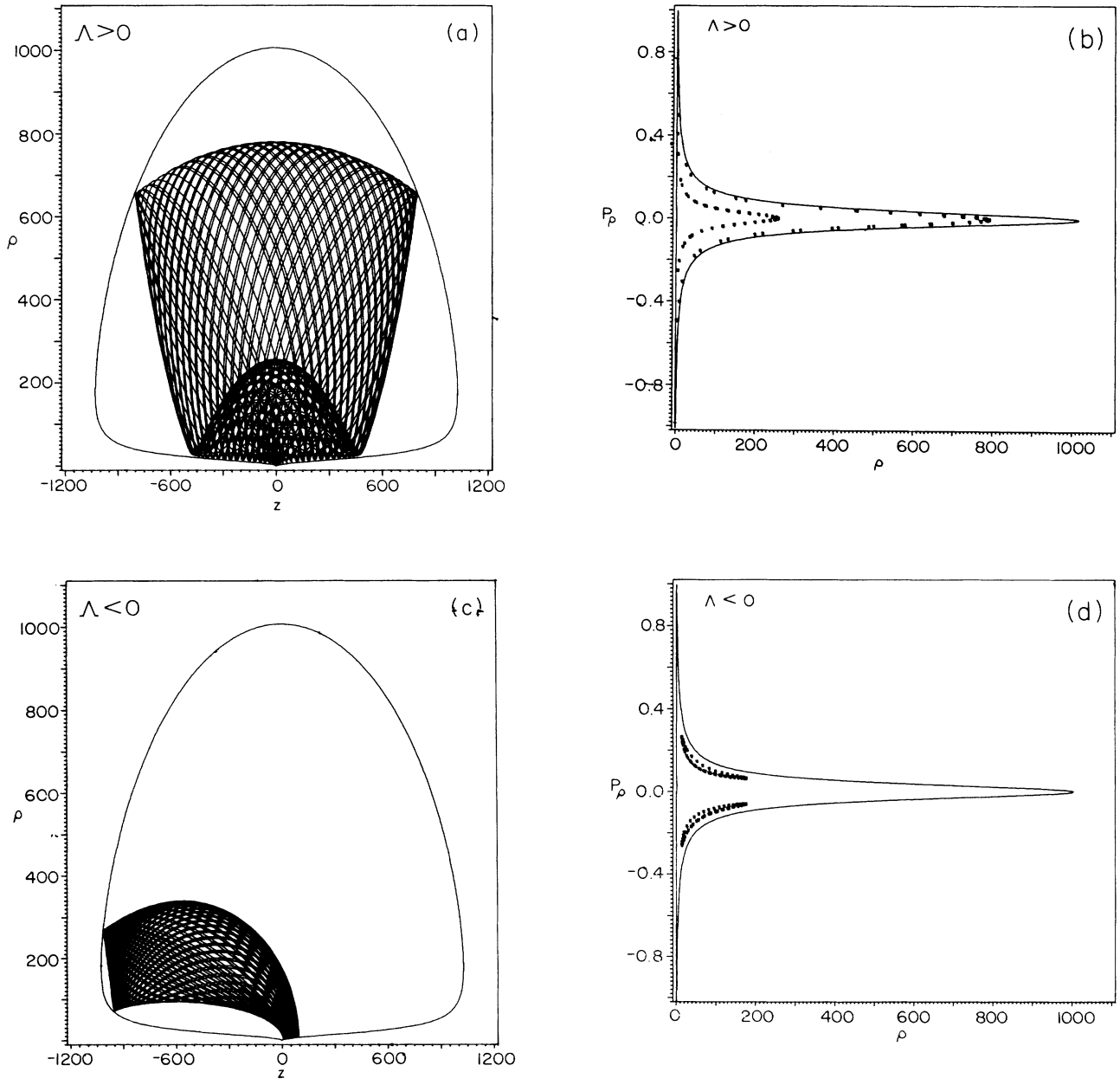

FIG. 2. Representative rotational and vibrational classical trajectories for the case $m=1$ together with their Poincaré surfaces of section. Frames (a) and (b) correspond to $\Lambda > 0$ and the trajectory is rotational while frames (c) and (d) correspond to $\Lambda < 0$ and the trajectory is vibrational; note that the second trajectory has a symmetry-related counterpart, obtained by reflection through the ρ axis. Both trajectories are at an energy $E = -9.327 \times 10^{-4}$.

is not an exact separation since n is not an exact quantum number).[103,104] Solov'ev's invariant Λ is the leading order term in the BGNF expression for the adiabatic invariant[86] (obtained in Ref. 18 for the special case that $m=0$). In Ref. 105 it was demonstrated that Padé resummation can be used to improve the convergence of the BGNF for coupled oscillator problems and work is currently underway to investigate the utility of this approach for the QZE. It is important to note that Λ is an *exact* constant of motion for the hydrogen atom and that a perfectly valid but nonstandard way of defining a "zeroth-order" quantum state is to diagonalize H_0, L_z, and Λ simultaneously. This will be exploited in the adiabatic-switching procedure discussed in Sec. III.

From the standpoint of semiclassical quantization it is clear from recent studies[72,74] that it is important to quantize the actions or combinations of actions which are the most appropriate to the various topologies exhibited by the classical trajectories. There are two distinct types of classical trajectory when $|m|=1$ (illustrated in Fig. 2) whose topology is determined by the sign of the approximate constant of motion Λ (see Ref. 6 for an excellent discussion of the classical mechanics of Λ). Note that Λ lies in the range $\Lambda_{\min} \le \Lambda \le \Lambda_{\max} = -1 \le \Lambda \le 4$. Trajectories with $\Lambda > 0$ are rotational, those with $\Lambda < 0$ are vibrational while those with $\Lambda = 0$ correspond to separatrix motion.[6,37,45,53,54,56–58,102] Interestingly, the consequences of the two types of dynamics have been observed in experimental studies of the QZE in lithium by Cacciani *et al.*[80] They studied a diamagnetic multiplet of odd Rydberg states and observed a transition from rigid-rotor-like spectra ($\Lambda > 0$) to anharmonically-coupled-oscillator-like behavior ($\Lambda < 0$). It is most noteworthy that they were able to correlate the change in behavior to the change in the sign of Λ whose value they obtained experimentally. Since Λ is not an *exact* constant of motion it is not strictly possible to define a trajectory with $\Lambda = 0$ because any trajectory starting out with initial conditions chosen so that $\Lambda = 0$ (separatrix motion) will eventually evolve into one or the other of the two families of trajectory, i.e., it may show either type of behavior, depending sensitively and unpredictably on the particular set of initial conditions. In the regular regime the classical mechanics of the QZE is qualitatively similar to that observed in resonant coupled oscillator systems where an exact constant of motion of H_0 (specifically, a generator of the appropriate Lie group[74]) may be approximately preserved in the coupled system, and serve to distinguish between the various families of classical trajectories. This can be understood by recognizing that the Kepler problem (or the hydrogen atom) is equivalent to a four-dimensional isotropic harmonic oscillator both classically[106–108] and quantum mechanically.[109,110] The QZE can therefore be formulated as four anharmonically coupled oscillators, with the special case of $m=0$ being reducible to a two-dimensional isotropic oscillator coupled by a polynomial perturbation as will be discussed in Sec. II A.[18,61,66] Based on the study of the classical trajectories in the QZE it seems reasonable by analogy that Λ would be the most appropriate variable to quantize in the QZE. This will be considered further in Sec. III.

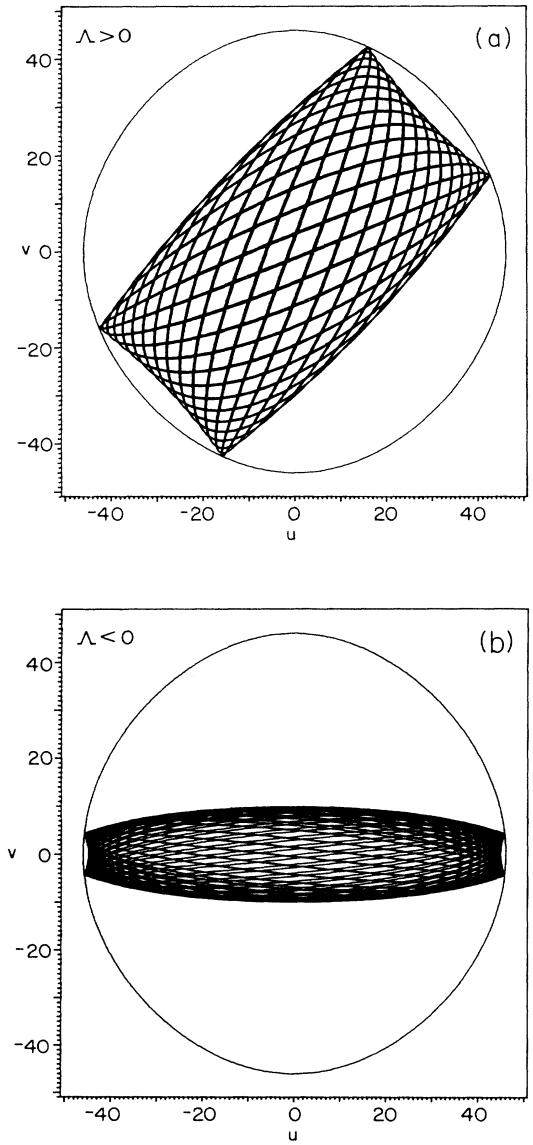

FIG. 3. Two trajectories, representative of the two families of trajectory with opposite values of Λ for the case $m=0$ in regularized coordinates, at $E=-9.439\times10^{-4}$.

The trajectories in Fig. 2 are typical of trajectories with $|m|>0$, but the $m=0$ case is more complicated since the centrifugal term is absent and therefore does not dominate the Coulomb term close to the origin; the Coulomb singularity makes it impractical to integrate the equations of motion in cylindrical coordinates. To deal with this problem the method of classical regularization[46,106] is used to remove the singularity via a transformation to squared parabolic coordinates,[4] as is now described.

A. Regularization of the QZE Hamiltonian when $m=0$

Unlike the case where $|m|>0$, if $m=0$ the centifugal term is absent in the classical Hamiltonian (2.1) and

the Coulomb singularity presents numerical problems when integrating Hamilton's equations. It is usual to circumvent this difficulty by employing the classical mechanical technique of regularization which involves both a coordinate and a time transformation.[106] When $m=0$ this can be accomplished by Levi-Civita's regularization in the plane[46,106] while the full problem (arbitrary m) is regularized using the method developed by Kustaanheimo and Steifel[108] which involves increasing the dimensionality of the problem from three to four in configuration space. In the present study, regularization is necessary only when $m=0$ and there is no need to perform the full Kustaanheimo-Steifel regularization.[108] The simpler Levi-Civita regularization is effected by first making a transformation to "squared" parabolic coordinates,[4,18,46,61,66,106]

$$\rho=uv, \quad z=(u^2-v^2)/2 , \tag{2.7}$$

in terms of which the Hamiltonian (2.1) becomes (setting $m=0$)

$$H=\frac{1}{2(u^2+v^2)}(P_u^2+P_v^2-4)+\frac{\gamma^2}{8}u^2v^2 , \tag{2.8}$$

giving on regularization[46,100]

$$K=2=\tfrac{1}{2}(P_u^2+P_v^2)-E(u^2+v^2)+\frac{\gamma^2}{8}u^2v^2(u^2+v^2) . \tag{2.9}$$

In the Hamiltonian K, the true energy of the QZE (i.e., E) occurs as a parameter while the physical trajectories evolve on an effective potential whose pseudoenergy is always equal to 2. This is equivalent to the approach used by Edmonds and Pullen[46] (see also Refs. 18 and 66). Note that the problem has been reduced to two isotropic (resonant) harmonic oscillators coupled by a polynomial perturbation. For this reason the classical trajectories resemble those of coupled oscillator problems of which there are numerous examples in the literature.[67–71] Again there are two distinct classes of trajectory according to the sign of the adiabatic invariant Λ, as illustrated in Fig. 3 (surfaces of section are displayed in Refs. 18 and 46). Trajectories with $\Lambda<0$ are localized along the u or the v axes and correspond to motion along the z axis in cylindrical coordinates. This family of trajectories ionizes if the energy is greater than $E_{\rm esc}$, along either of the two equivalent valleys on the potential energy surface shown in Ref. 18. The second family of trajectories corresponds to motion along the potential ridge discussed by Fano[59,60] and by Clark and Taylor (who illustrate the ridge in polar coordinates[52]). These trajectories are concentrated along the lines $u=v$ which is equivalent to motion chiefly along the ρ axis in cylindrical coordinates. [Note that the choice of coordinates in Eq. (2.7) differs from those used in Refs. 18 and 46. The potential energy surface in the present coordinates is related to that in Refs. 18 and 46 by a rotation through 45° The coordinates in Eq. (2.7) correspond to the more usual definition of squared parabolic coordinates.[4]] The quasi-Landau spacings may be obtained by quantizing trajectories lying exclusively along the potential ridge[46–51] (i.e., along the ρ axis), and consequently trajectories with $\Lambda\approx\Lambda_{\max}$ are relevant to understanding the quasi-Landau resonances. Examination of classical trajectories (Fig. 3) and surfaces of section for the $m=0$ case in Ref. 18 revealed that the volumes of phase space corresponding to $\Lambda<0$ are more prone to chaos than are those volumes where $\Lambda>0$. Contour plots of Λ for $m=0$ are compared with numerically determined Poincaré surfaces of section in Ref. 18 (in squared parabolic coordinates) and it is unnecessary to reproduce them here. It is important to note that the transformation to regularized coordinates is primarily for computational reasons and that the *sign* of Λ still governs the topology of the trajectories whatever the value of m. For this reason, in the AS procedure for the QZE, a zeroth-order torus is determined by diagonalizing the quantum operators corresponding to H_0 and Λ simultaneously, as will now be discussed.

III. ADIABATIC SWITCHING

The basic idea of AS is due to Ehrenfest[111] but the method was first developed and applied by Solov'ev[87] with the first practical application to a realistic problem by Grozdanov and Solov'ev[88] who treated the hydrogen atom in crossed electric and magnetic fields. Although highly significant, this latter application was rather limited in scope, dealing only with three very-low-lying states whose energies corresponded to highly regular classical dynamics. Recently there has been renewed interest in AS for *model* molecular Hamiltonians[89–95] but the present study of the QZE represents the first comprehensive application of the method to a realistic physical system. After giving a brief outline of the time-dependent AS method, specific application to the QZE is made.

In time-dependent AS the nonintegrable Hamiltonian is first written in the form

$$H(t)=H_0+\epsilon(t)H_1 , \tag{3.1}$$

where H_0 is an integrable (usually but not necessarily separable) zeroth-order approximation to the full Hamiltonian and H_1 is a perturbation which need not be small. The function ϵ(t) is a time-dependent switching function which is chosen to vary slowly and smoothly from 0 to 1 over the course of the switching time T, so that at time $t=T$, $\epsilon(t)=1$ and the perturbation is fully turned on. A comprehensive study of the best choice of switching function has been made by Johnson.[90]

A zeroth-order classical torus may be defined by specifying a set of actions for H_0 and these values can then be used to generate the initial conditions needed to integrate the equations of motion for $H(t)$. Along a trajectory, if adiabatic invariance holds, the adiabatic invariant will be preserved provided the perturbation is turned on sufficiently slowly but because the energy is not itself an adiabatic invariant its value will change as a function of time. If the zeroth-order torus is chosen to correspond to a quantum state of H_0 at the end of the switching (i.e., at $t=T$) the zeroth-order torus will have distorted into a quantized torus of the full Hamiltonian

with the appropriate quantized energy. In essence the method follows the highly nonlinear evolution of a torus of H_0 into a torus of the full Hamiltonian. Clearly not all quantized choices of zeroth-order tori will necessarily evolve into quantized tori of the full Hamiltonian because not all actions or combinations of actions are adiabatic invariants. The method thus requires some insight into which quantities are approximately conserved in the full Hamiltonian. A zeroth-order torus can then be specified by quantizing the energy and the other conserved or *approximately conserved* quantities. The most appropriate *zeroth-order* torus is therefore determined by the topologies of the classical trajectories of the *full* Hamiltonian. If H_0 is resonant (degenerate) there is some ambiguity in defining a zeroth-order torus just as in the corresponding degenerate quantum system more than one eigenfunction corresponds to a particular eigenvalue. The hydrogen atom is highly degenerate: its spherical symmetry is responsible for the degeneracy with respect to m, while the existence of the Runge-Lenz vector as an "extra" constant of motion, due to the particular form of the Coulomb potential, gives rise to the orbital degeneracy.[112] Based on the classical study presented in Sec. II it is clear that the best zeroth-order tori from the point of view of AS will be those defined by simultaneously diagonalizing the quantum operator corresponding to H_0 and Λ. The quantization of Λ has been the subject of recent semiclassical[54] and quantum studies.[16,56] Because it is easier to perform a quantum-mechanical diagonalization of Λ than to effect a semiclassical quantization, quantum values of Λ are used to define the zeroth-order tori (details are given in the Appendix). Once a zeroth-order torus has been specified, initial conditions for integrating the equations of motion for $H(t)$ must then be generated as is now described.

A. Calculation of initial conditions

For fixed values of m, phase space is four dimensional and quantizing E and Λ restricts the dynamics of H_0 to the surface of a two-dimensional torus embedded in this phase space. Points on the torus correspond to initial conditions for classical trajectories all having the same values of E and Λ. In principle, as the switching time $T\rightarrow\infty$ the energy of any trajectory starting out on the initial torus should converge to the correct final quantized value. It is obviously not possible to integrate trajectories for infinite times so, in practice, an ensemble of trajectories starting out on the same initial torus is propagated forward in time, with initial conditions chosen uniformly and randomly on the surface of the torus. In effect, this approach propagates the entire torus forward in time. As pointed out by Solov'ev[87] and others[90,91,93,94] this tactic, combined with averaging over the final energies, not only accelerates the convergence but can also compensate for nonadiabatic effects. After averaging, the standard deviation of the energies is used as an indicator of the accuracy of the method and in this sense the method is self-diagnostic.

To generate initial conditions, the energy and the classical adiabatic invariant Λ are first expressed in cylindrical coordinates,

$$E=E(\rho,P_\rho,z,P_z)\ , \tag{3.2}$$

$$\Lambda=\Lambda(\rho,P_\rho,z,P_z)\ . \tag{3.3}$$

For quantized E and Λ these equations are used to generate initial conditions ρ^0, P_ρ^0, z^0, and P_z^0. In general, an analytical solution is not possible so the following strategy is employed.

(1) Set $z=P_\rho=P_z=0$; Eq. (3.2) is then solved numerically for ρ. Two values, $\rho^{\min}$ and $\rho^{\max}$ are obtained and the initial condition ρ^0 is selected uniformly and randomly between these values.

(2) Setting $\rho=\rho^0$ and $P_z=P_\rho=0$, Eq. (3.2) is solved for z, again giving maximum and minimum values $z^{\min}$ and $z^{\max}$ in which range z^0 is selected uniformly and randomly. The values $\rho^{\min}$, $\rho^{\max}$, $z^{\min}$, and $z^{\max}$ correspond to points on the equipotential in configuration space. Note that $z^{\min}$ and $z^{\max}$ are both functions of ρ^0.

(3) Using ρ^0 and z^0 Eqs. (3.2) and (3.3) are solved *simultaneously* for P_z^0 and P_ρ^0. Although the points ρ^0 and z^0 lie on the energy shell, they do not necessarily lie on the surface defined by the intersection of the energy shell and the surface of constant Λ in which case the values of P_ρ^0 and/or P_z^0 obtained will be complex; in this event the entire procedure is repeated until physically acceptable initial conditions are obtained. Since the equations can be reduced to polynomials in coordinates and momenta, efficient numerical routines for solving polynomials may be used to advantage.

The application of AS to the $m=0$ and $|m|>0$ cases is fundamentally different and so the two cases are discussed separately; since the $|m|>0$ case is the more straightforward it is described first.

B. Time-dependent adiabatic switching when $|m|>0$

The Hamiltonian (2.1) is split up in the following way:

$$H(t)=H_0+\epsilon(t)H_1\ , \tag{3.4}$$

where,

$$H_0=\tfrac{1}{2}(P_\rho^2+P_z^2)+\frac{m^2}{2\rho^2}-\frac{1}{(\rho^2+z^2)^{1/2}} \tag{3.5}$$

and

$$H_1=\frac{\gamma^2}{8}\rho^2 \tag{3.6}$$

with the switching function being given by

$$\epsilon(t)=\frac{t}{T}-\frac{\sin(2\pi t/T)}{2\pi}\ ,\quad 0\le t\le T\ . \tag{3.7}$$

This particular form of switching function has been used extensively in previous AS calculations.[89–94]

In Table I are presented semiclassical eigenvalues calculated using AS for states in the manifold $n=23$ at a magnetic field strength of 4.7 T corresponding to $\gamma=2.0\times10^{-5}$. Also given in Table I are quantum variational results calculated by Clark and Taylor who diagonalized the Hamiltonian using a Sturmian basis,[21,22,52] together with the second-order quantum-perturbation re-

TABLE I. Energy eigenvalues for states in the $n=23$ manifold, with $m=1$, for $\gamma=2\times10^{-5}$ and $T=1.0\times10^{6}$. The paramagnetic energy Eq. (2.3b) has been included ($s_z=0$). Λ is the quantized value of the *classical* adiabatic invariant, E^{QM} the exact quantum variational results (Ref. 22), E^{PT} the second-order quantum-perturbation-theory results (Ref. 16), E^{AS} the adiabatic switching results (average of 25 different trajectories), and ΔE^{AS} the standard deviations of the adiabatic switching results.

r	Λ	$-E^{\mathrm{QM}}\times10^{4}$	$-E^{\mathrm{PT}}\times10^{4}$	$-E^{\mathrm{AS}}\times10^{4}$	ΔE^{AS}
0	−0.642 083 6	9.326 596	9.326 608	9.326 972	3.10×10^{-5}
1	−0.642 083 3	9.326 596	9.326 608	9.326 974	3.30×10^{-5}
2	−0.327 673 7	9.304 868	9.304 888	9.305 336	1.39×10^{-4}
3	−0.327 463 3	9.304 857	9.304 877	9.305 279	1.59×10^{-4}
4	−0.086 134 6	9.287 976	9.287 986	9.288 688	2.68×10^{-4}
5	−0.069 497 5	9.287 006	9.287 035	9.287 517	3.20×10^{-4}
6	0.067 589 3	9.277 405	9.277 446	9.278 114	3.57×10^{-4}
7	0.171 828 2	9.270 574	9.270 631	9.271 084	2.54×10^{-4}
8	0.313 651 4	9.260 995	9.261 069	9.261 469	1.76×10^{-4}
9	0.474 267 6	9.250 151	9.250 244	9.250 559	1.63×10^{-4}
10	0.654 329 4	9.237 967	9.238 081	9.238 286	1.85×10^{-4}
11	0.852 813 3	9.224 520	9.224 659	9.224 768	2.69×10^{-4}
12	1.069 270	9.209 840	9.210 007	9.209 936	3.14×10^{-4}
13	1.303 409	9.193 947	9.194 146	9.194 015	3.70×10^{-4}
14	1.555 037	9.176 853	9.177 088	9.176 868	4.40×10^{-4}
15	1.824 021	9.158 565	9.158 839	9.158 590	5.12×10^{-4}
16	2.110 266	9.139 087	9.139 406	9.139 074	4.63×10^{-4}
17	2.413 702	9.118 421	9.118 790	9.118 240	3.81×10^{-4}
18	2.734 279	9.096 569	9.096 994	9.096 488	3.82×10^{-4}
19	3.071 957	9.073 531	9.074 016	9.073 508	2.49×10^{-4}
20	3.426 705	9.049 305	9.049 858	9.049 485	1.80×10^{-4}
21	3.798 501	9.023 891	9.024 571	9.024 215	1.38×10^{-4}

sults of Grozdanov and Taylor.[16] Each AS eigenvalue is the result of averaging 25 final energies obtained by integrating the equations of motion for $H(t)$ using the switching function in Eq. (3.7) with $T=1.0\times10^{6}$. Also listed are the calculated standard deviations.

In Table I each state is labeled by three quantum numbers, n, m, and r, where r is an ordinal diagonalization index (described in the Appendix) and which can be interpreted as the number of nodes of the wave function corresponding to the state $|nrm\rangle$ along one of the elliptical cylindrical coordinate axes on the Fock hypersphere in momentum space.[16,56] The results in Table I correspond to the "weak field" limit where $\gamma n^{3}\ll1$ and inter-n mixing can be neglected, i.e., n is still a good quantum number, although note that the only *exact* quantum number is m. It is apparent on examination of Table I that the AS results are in excellent agreement with the quantum-variational results for all of the states in the manifold. For the lowest states the perturbation results are in slightly better agreement with exact quantum results than are the AS eigenvalues. However, the standard deviations for the AS results are consistently small for the entire manifold, and, in contrast to perturbation theory, the AS eigenvalues actually improve as a function of increasing energy. This observation may be explained by considering the change in the localization of the classical trajectories as energy increases within the manifold. Specifically, states with values of r such that $\Lambda<0$ (i.e., $0\le r\le5$) are vibrational while those with values of r such that $\Lambda>0$ (i.e., $6\le r\le21$) are rotational, with the low-lying states in the manifold being strongly localized along the z axis while the high-lying states are strongly localized along the ρ axis (see Fig. 4). At this point it is also relevant to note that in the regime where $\gamma^{2}n^{7}\ll1$ (the inter-l mixing regime) Delande and Gay[6] using first-order degenerate quantum-perturbation theory have shown that the wave functions $\langle\mathbf{r}\,|\,n,r,m\rangle$ have different localization properties determined by the quantum number $\mathbf{r}$, which is consistent with Fig. 4. Richards[65] parameterized the problem as a double-well potential using first-order classical perturbation theory; in this picture the vibrational states occur as almost degenerate pairs below the barrier top while the rotational states lie above the barrier top (the barrier top itself corresponds to the separatrix). The eigenvalues in Table I clearly fit this picture. As noted, the AS procedure is consistently able to quantize the higher rotational states slightly better than the vibrational states. The vibrational states are on average closer in energy to the separatrix than are the higher rotational states and consequently vibrational trajectories are more likely to encounter high-order resonances. The study of classical trajectories and Poincaré surfaces of section in Ref. 18 revealed that Λ is a better approximate constant of motion for rotational states than for vibrational states, or, stated differently, the vibrational volumes of phase space are more prone to chaos than are the rotational parts of phase space. The highly localized rotational states are farthest from the separatrix and this is reflected in the better accuracy of the AS eigenvalues for these states; this is a relatively small effect in the $n=23$ manifold for this field strength. This could have an important consequence; even in the

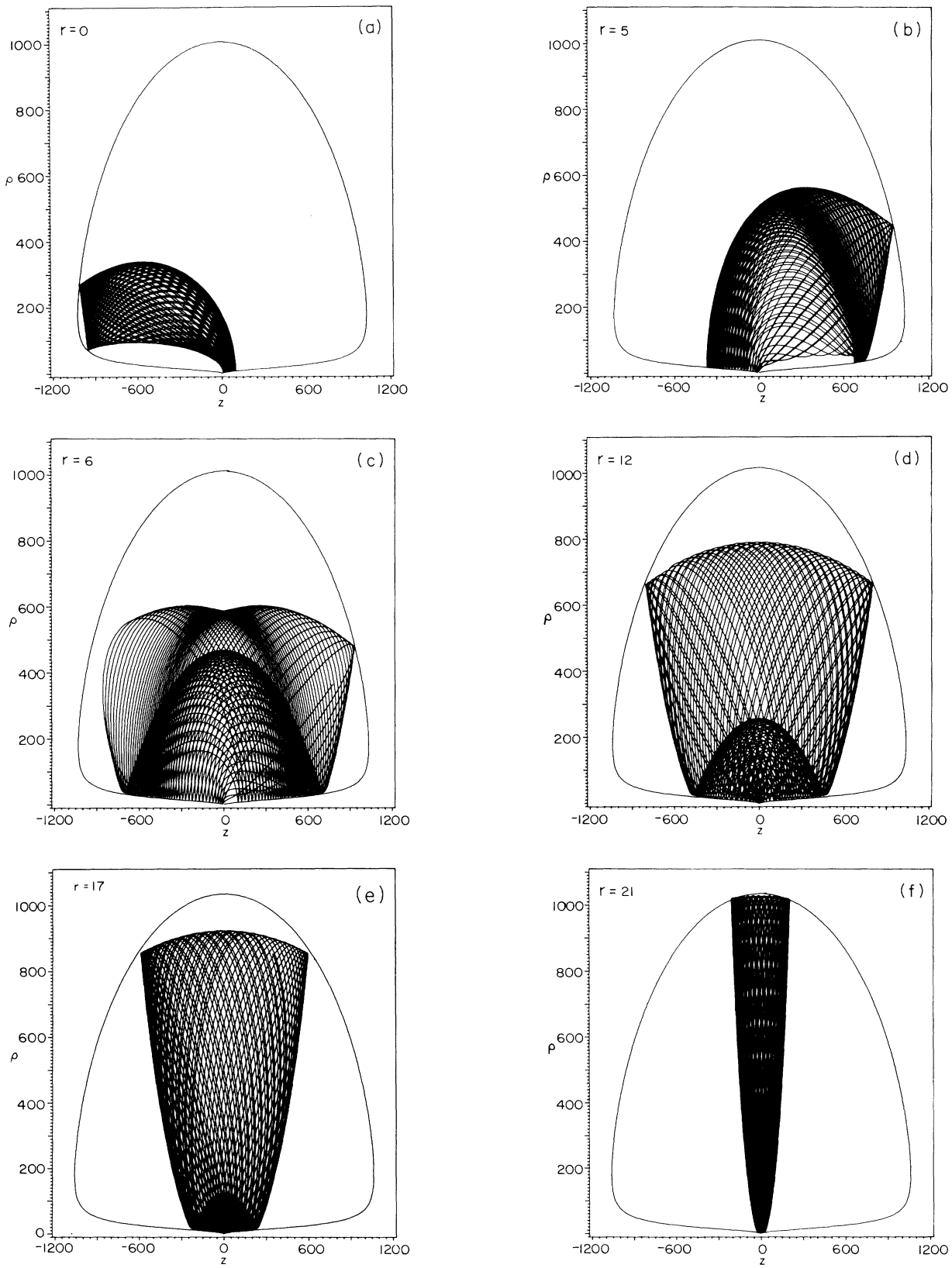

FIG. 4. Typical quantized trajectories obtained using AS corresponding to the states in Table I (i.e., the $n=23$ manifold with $m=1$). The value of the quantum number r is displayed in each frame. Note that the trajectories with $r=5$ and 6 are on opposite sides of the separatrix. The rotational state with $r=21$ is strongly localized along the ρ axis.

strongly chaotic volumes of phase space, these ridge states probably persist and their identification semiclassically could facilitate the assignment of the quantum spectrum.

It is useful to examine the final quantized trajectories obtained by AS for a few of the states in Table I. These trajectories are obtained in the following manner: after adiabatic switching is complete (i.e., the perturbation is fully turned on), the equations of motion continue to be integrated with $\epsilon(t)=1$ for all subsequent times $t \geq T$. This is equivalent to integrating Hamilton's equations for the full Hamiltonian using as initial conditions the values of coordinates and momenta obtained at the conclusion of adiabatic switching. Figure 4 illustrates the transition from vibrational to rotational motion as a function of the quantum number r. The trajectory with $r=0$ is strongly localized along the z axis which would indicate that the wave function should also be strongly localized along the z axis (see the discussion of Hose *et al.*[113] using the Hellmann-Feynman theorem and also the arguments made by Richards[65]). The trajectories which are chosen to illustrate states with $r=5$ and 6 (where the transition in the sign of Λ occurs) are both close to but on opposite sides of the separatrix and this is reflected in the local maximum observed in the standard deviations around this point. The consequent deformations in the topologies of the trajectories is clearly seen in Figs. 4(b) and 4(c). The high lying rotational trajectories with $17 \leq r \leq 21$ are localized along the ρ axis and correspond to states lying along the potential "ridge" discussed by Fano[59,60] (the ridge is apparent if the potential is plotted in spherical coordinates and is illustrated by Clark and Taylor in Ref. 52). In order to emphasize the importance of choosing a zeroth-order torus specified by quantizing E and Λ, results obtained by using initial conditions lying on a surface of a torus defined by quantizing A_z rather than Λ were also performed. For low-lying vibrational states $A_z \approx -\Lambda$ and the two sets of AS results were in good agreement, as expected, since A_z is a good approximate constant of motion for vibrational trajectories corresponding to low values of r.[6,56] However, the two sets of AS results diverged noticeably for the rotational states, which underscores the necessity of quantizing actions or operators appropriate to *both* of the observed topologies of the classical trajectories.[72–74]

In Table II AS results are compared with exact quantum-variational calculations and second-order quantum-perturbation results for states in the manifolds $n=2$, 3, and 4 for a considerably higher field than in Table I, i.e., $\gamma=0.01$ (corresponding to a field of 2.35×10^3 T) which combination is still, however, in the regime $\gamma n^3 \ll 1$. For this value of n there are no vibrational states, in agreement with the condition obtained by Solov'ev,[53,54] Richards,[65] and also by Coffey *et al.*[86] who showed that vibrational states exist (based on first-order classical perturbation theory) only if $m < n/\sqrt{5}$. Some of the trends observed in Table I are also apparent in Table II. States close to the separatrix display larger-than-normal standard deviations, but the standard deviations are certainly acceptable and the AS results are in excellent agreement with exact quantum results. Representative quantized trajectories for most of the states are shown in Fig. 5.

In order to test the usefulness of the criterion $\gamma n^3 \ll 1$ as a way of estimating when AS will be useful, in Table III results are presented for selected states in the $n=2$, 3, and 4 manifolds for the higher magnetic field of 2.35×10^4 T for which $\gamma=0.1$. It is reasonable to expect that in practice AS may perform well even when the criterion in Eq. (2.6) is not obeyed since Λ is only a *first-order* approximation to the adiabatic invariant of the full QZE. The advantage of AS is that a high-order representation for the adiabatic invariant is not needed explicitly, i.e., the method "senses" the existence of such an invariant. Examination of the standard deviations indicates that while adiabatic invariance is being violated, the results themselves are in acceptable but not outstanding agreement with quantum-variational calculations. While this is consistent with the findings of other studies that AS can be extended into mildly chaotic volumes of classical phase space, the results seem to indicate that in the QZE invariance of Λ itself is a prerequisite for AS to work. Note that all but the lowest state in Table III [i.e., $(n,m,r)=(2,-1,0)$] are in chaotic volumes of classical phase space as is clearly seen on ex-

TABLE II. Energy eigenvalues for $\gamma=0.01$ and a switching time $T=6.0\times10^4$ except $n=2$, $m=-1$ for which $T=1.0\times10^4$. Note that the paramagnetic energy has been included ($s_z=-\frac{1}{2}$). Λ is the quantized value of the classical adiabatic invariant, E^{QM} the exact quantum-variational results (Ref. 24), E^{PT} the second-order quantum-perturbation-theory results (Ref. 16), E^{AS} the adiabatic switching results (average of 25 different trajectories), and ΔE^{AS} the standard deviations of the adiabatic switching results.

n	m	r	Λ	$-E^{\mathrm{QM}}\times10^4$	$-E^{\mathrm{PT}}\times10^4$	$-E^{\mathrm{AS}}\times10^4$	ΔE^{AS}
2	−1	0	1.000 000 00	0.134 701 0	0.134 701 0	0.134 776 0	3.7×10^{-8}
3	−2	0	0.888 888 89	0.069 247 2	0.069 251 8	0.069 402 2	1.7×10^{-7}
3	−1	0	0.333 333 33	0.064 678 1	0.064 680 2	0.064 838 2	5.0×10^{-8}
3	−1	1	2.111 111 11	0.063 820 1	0.063 827 5	0.063 971 9	3.5×10^{-7}
4	−3	0	0.750 000 00	0.047 707 6	0.047 919 9	0.047 926 3	8.2×10^{-7}
4	−2	0	0.437 500 00	0.043 552 7	0.043 672 4	0.043 791 3	1.0×10^{-6}
4	−2	1	1.937 500 00	0.041 571 0	0.041 922 6	0.041 778 3	1.9×10^{-6}
4	−1	0	0.094 131 15	0.039 275 5	0.039 333 7	0.039 522 0	3.2×10^{-6}
4	−1	1	1.000 000 00	0.038 132 2	0.038 332 2	0.038 345 9	2.7×10^{-6}
4	−1	2	2.655 868 80	0.035 871 5	0.036 301 0	0.036 0731	3.3×10^{-6}

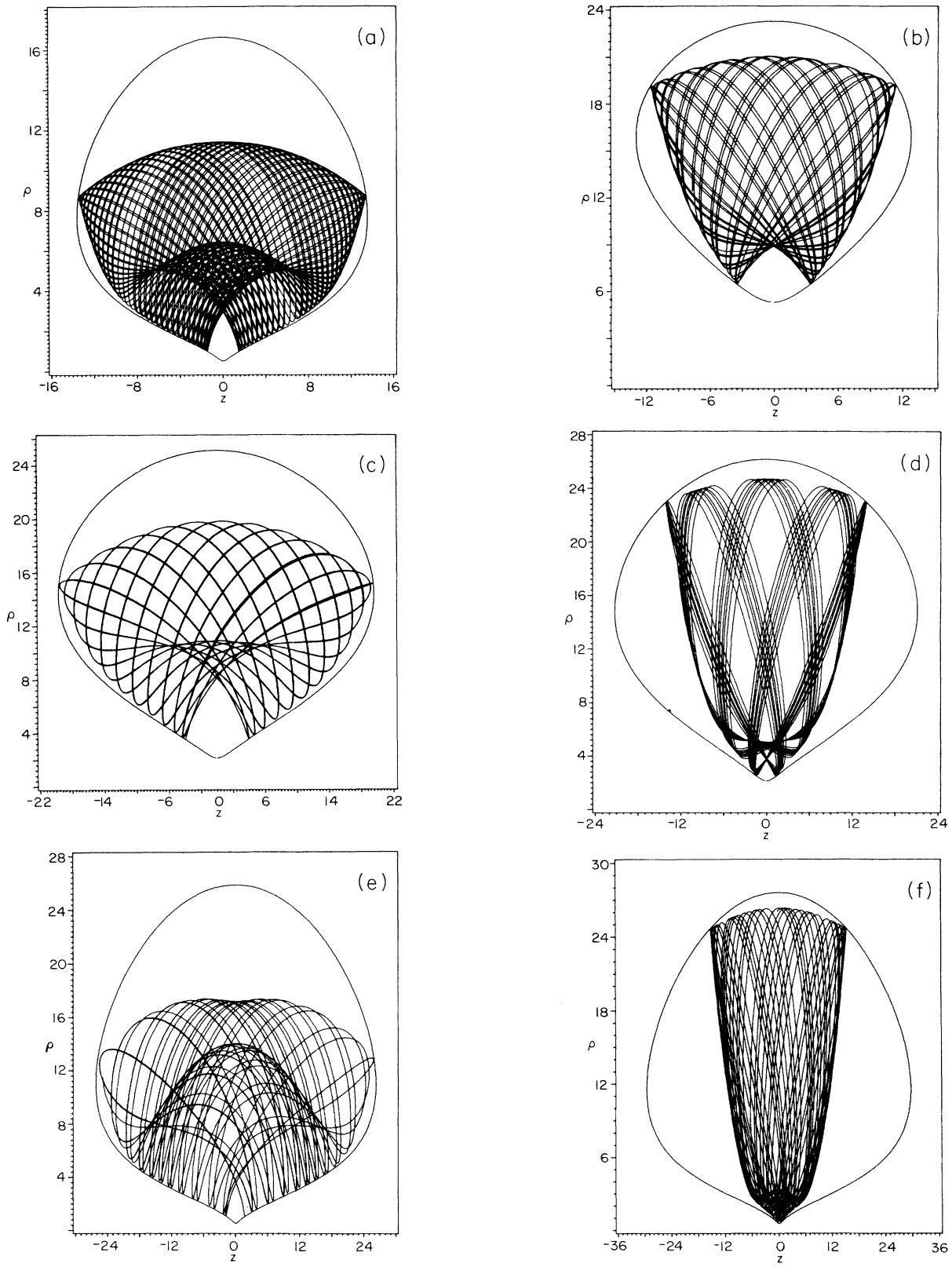

FIG. 5. Representative quantized trajectories obtained using AS for some of the states in Table II. The trajectories are reminiscent of those for anharmonically coupled oscillator problems. The trajectory in frame (c) has evidently finished up in a low-order resonance zone. The states are labeled (n,m,r) as follows: (a) $(3,-1,0)$, (b) $(4,-3,0)$, (c) $(4,-2,0)$, (d) $(4,-2,1)$, (e) $(4,-1,0)$, (f) $(4,-1,0)$.

TABLE III. Energy eigenvalues for $\gamma=0.1$ and the switching $T=1.0\times10^4$. The paramagnetic energy has been included ($s_z=-\frac{1}{2}$). E^{QM} are the quantum variational results (Ref. 24), E^{AS} the adiabatic switching results (average of 25 trajectories), and ΔE^{AS} the standard deviations for the adiabatic switching results.

n	m	r	$-E^{QM}$	$-E^{AS}$	ΔE^{AS}
2	−1	0	0.200 840 6	0.205 983 2	1.3×10^{-5}
3	−2	0	0.137 839 5	0.145 472 4	8.7×10^{-4}
4	−3	0	0.111 860 2	0.120 086 5	1.3×10^{-3}
3	−1	1	0.107 812 1	0.112 919 7	9.0×10^{-4}
3	−1	0	0.082 110 8	0.094 618 9	2.2×10^{-3}
4	−2	1	0.081 171 2	0.090 979 8	1.8×10^{-3}
4	−2	0	0.063 317 6	0.073 767 5	3.1×10^{-3}
4	−1	0	0.053 245 6	0.064 293 6	2.5×10^{-3}

amination of final quantized trajectories (illustrated in Fig. 6). It is interesting to observe the tendency of the trajectories with larger values of r to spiral along the z axis [Figs. 6(e) and particularly 6(f)]. These trajectories, whose topology is evidently different from the rotational and vibrational trajectories observed previously would eventually ionize in the z direction if the energy were higher than E_{esc}. For these states there is a clear separation of frequencies between that in the z direction and that in the ρ direction and it seems likely that the method applied by Noid *et al.*[64] based on the classical Born-Oppenheimer approximation would be appropriate for these states.

C. Time-independent adiabatic switching when $m=0$

In this section a new development in the theory of AS is described, namely, time-independent AS in extended classical phase space. As noted, the Coulomb singularity when $m=0$ makes it impractical to integrate the equations of motion in cylindrical coordinates. While parabolic coordinates are convenient for integrating Hamilton's equations they do not lend themselves directly to the AS method. Referring to Eq. (2.9), note that the true energy E occurs as a parameter in the Hamiltonian K and that the dynamics for *all* values of the perturbation must lie on the pseudoenergy shell $K=2$ if the trajectories of the regularized Hamiltonian are to correspond to physical trajectories of the QZE. Introduction of any time dependence into the Hamiltonian K via a switching function would immediately move the system off of the pseudoenergy shell. In order to constrain the dynamics to the surface $K=2$, an explicit time dependence would have to be introduced into E to compensate for the time dependence in the switching function. This is not feasible since, in essence, it is precisely the response of the eigenvalue E to the change in the switching function which is being elicited. This problem is solved by working in extended phase space[102] which leads to the development of time *independent* AS.

Introducing the switching function $\epsilon(t)$ into the Hamiltonian (2.8) gives

$$H=\frac{1}{2(u^2+v^2)}(P_u^2+P_v^2-4)+\epsilon(t)\frac{\gamma^2}{8}u^2v^2 \ . \tag{3.8}$$

This Hamiltonian still contains a singularity when $u=v=0$ and so AS cannot be performed directly using Eq. (3.8). However, a Hamiltonian suitable for AS can be obtained by first eliminating the time dependence in Eq. (3.8) by a transformation to extended phase space, followed by a regularization.[106] The canonical transformation to extended phase space is given by[101]

$$P_\theta=-E(=-H), \quad \theta=t \tag{3.9}$$

with the new Hamiltonian H being related to the old by

$$\bar{H}=H+P_\theta=0 \ , \tag{3.10}$$

or, explicitly,

$$\bar{H}=0=\frac{1}{2(u^2+v^2)}(P_u^2+P_v^2-4)+\epsilon(\theta)\frac{\gamma^2}{8}u^2v^2+P_\theta \ . \tag{3.11}$$

The old time and the old energy (i.e., $-E$) are now treated like any other pair of canonical coordinates and momenta in the extended six-dimensional phase space. The new Hamiltonian given by Eq. (3.11) does not explicitly depend on time; flow in the extended phase space is parameterized by a new "time" ζ which does not appear in the Hamiltonian. The Hamiltonian (3.11) can now be regularized to give

$$\bar{K}(\theta)=2=\tfrac{1}{2}(P_u^2+P_v^2)+P_\theta(u^2+v^2)+\epsilon(\theta)\frac{\gamma^2}{8}u^2v^2(u^2+v^2) \ , \tag{3.12}$$

where the switching function $\epsilon(\theta)$ is given by

$$\epsilon(\theta)=\frac{\theta}{\Theta}-\frac{\sin(2\pi\theta/\Theta)}{2\pi} \ , \quad 0\le\theta\le\Theta \ . \tag{3.13}$$

The equations of motion for Eq. (3.12) are simply Hamilton's equations of motion in the six-dimensional extended phase space. The initial conditions are generated in exactly the same way as for $|m|>0$, in cylindrical coordinates, and are then transformed into parabolic coordinates in extended phase space using Eq. (2.7) with the additional initial conditions

$$\theta^0=0 \text{ and } P_\theta^0=-1/(2n^2) \ , \quad n=1,2,3\ldots . \tag{3.14}$$

Along a trajectory in the six-dimensional phase space,

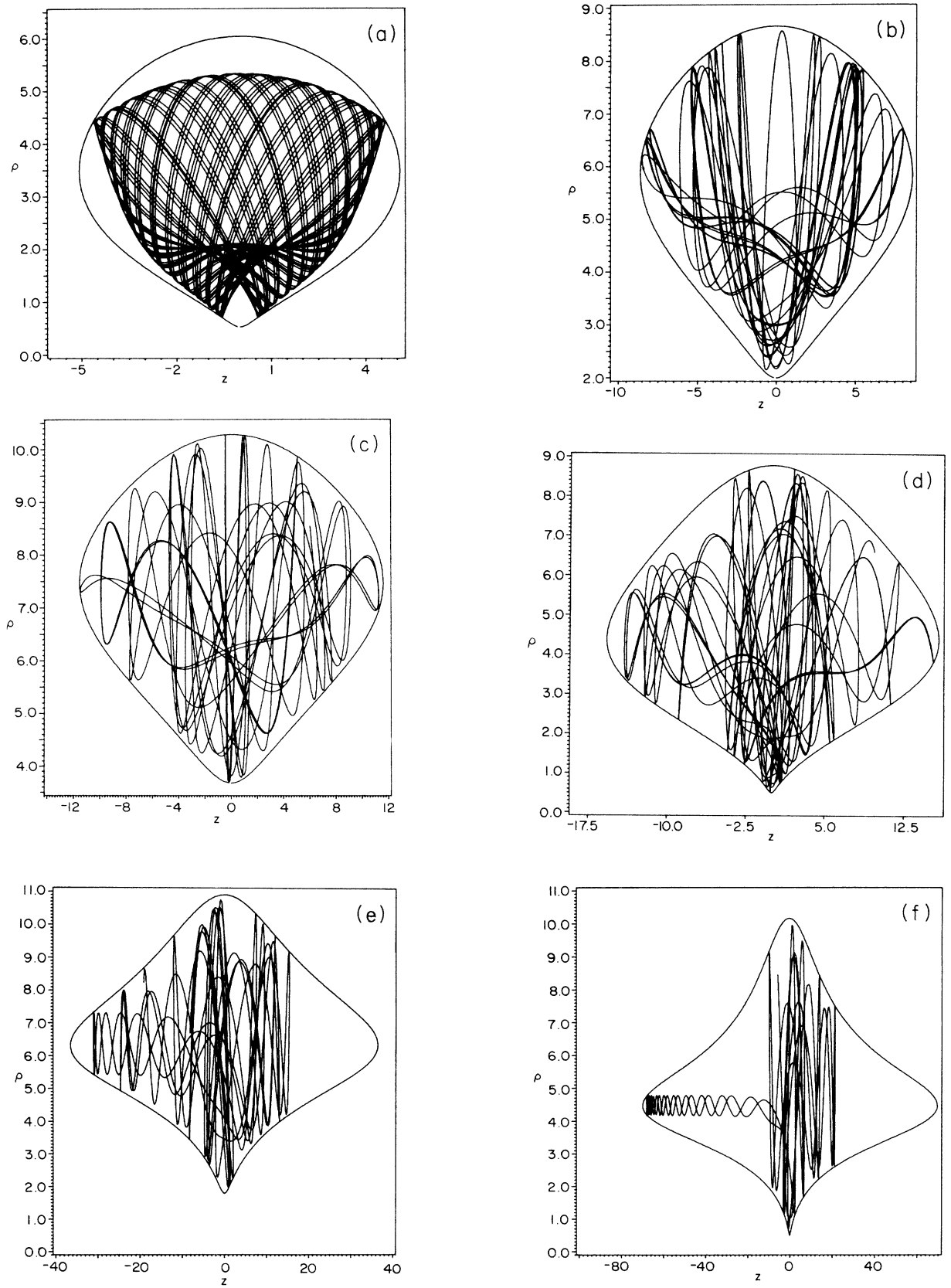

FIG. 6. Representative quantized trajectories obtained using AS for some of the states in Table III. The states are labeled (n,m,r) as follows: (a) $(2,-1,0)$, (b) $(3,-2,0)$, (c) $(4,-3,0)$, (d) $(3,-1,1)$, (e) $(4,-2,0)$, (f) $(4,-1,0)$.

TABLE IV. Energy eigenvalues for states in the $n=23$ manifold with $m=0$, $\gamma=2.0\times10^{-5}$, and $T=1.0\times10^{6}$. Λ is the quantized value of the classical adiabatic invariant, E^{QM} the exact quantum variational results (Ref. 21), E^{PT} the second-order quantum-perturbation-theory (Ref. 16), E^{AS} the adiabatic switching results, and ΔE^{AS} the standard deviations for the adiabatic switching results.

r	Λ	$-E^{\mathrm{QM}}\times10^{4}$	$-E^{\mathrm{PT}}\times10^{4}$	$-E^{\mathrm{AS}}\times10^{4}$	ΔE^{AS}
0	−0.815 178	9.438 674	9.438 681	9.439 057	1.7×10^{-6}
1	−0.815 178	9.438 674	9.438 681	9.439 057	1.6×10^{-6}
2	−0.474 465	9.415 159	9.415 176	9.415 557	3.3×10^{-5}
3	−0.474 452	9.415 158	9.415 176	9.415 556	3.3×10^{-5}
4	−0.191 242	9.395 521	9.395 539	9.395 977	9.9×10^{-5}
5	−0.188 600	9.395 375	9.395 399	9.395 779	9.7×10^{-5}
6	−0.006 502	9.382 497	9.382 515	9.383 111	2.4×10^{-4}
7	0.050 734	9.378 911	9.378 952	9.379 238	1.6×10^{-4}
8	0.179 022	9.370 168	9.370 228	9.370 617	9.3×10^{-5}
9	0.317 834	9.360 855	9.360 929	9.361 249	4.5×10^{-5}
10	0.479 349	9.349 941	9.350 035	9.350 318	3.7×10^{-5}
11	0.659 818	9.337 729	9.337 844	9.338 088	4.3×10^{-5}
12	0.858 665	9.324 257	9.324 397	9.324 605	6.6×10^{-5}
13	1.075 54	9.309 556	9.309 724	9.309 882	8.8×10^{-5}
14	1.309 82	9.293 645	9.293 845	9.293 954	1.1×10^{-4}
15	1.561 67	9.276 536	9.276 771	9.276 852	1.2×10^{-4}
16	1.830 84	9.258 234	9.258 509	9.258 555	1.3×10^{-4}
17	2.117 24	9.238 744	9.239 064	9.239 022	9.7×10^{-5}
18	2.420 82	9.218 068	9.218 438	9.218 394	1.2×10^{-4}
19	2.741 15	9.196 207	9.196 632	9.196 542	1.1×10^{-4}
20	3.079 30	9.173 161	9.173 647	9.173 465	6.4×10^{-5}
21	3.434 14	9.148 928	9.149 482	9.149 278	5.6×10^{-5}
22	3.806 02	9.123 507	9.124 135	9.123 861	1.9×10^{-5}

P_θ ($=-E$) and θ ($=t$) evolve like any other pair of conjugate coordinates and momenta. At the end of the integration when $\theta=\Theta$ (the precise end point is obtained using interpolation) the quantized value of the energy is given by $E=-P_\theta$. The equation of motion for θ is

$$\dot{\theta}=\frac{d\theta}{d\xi}=\frac{\partial\bar{K}}{\partial P_\theta}=(u^2+v^2) \tag{3.15}$$

with θ clearly a monotonically increasing function of ξ. Although the dimensionality of the system has been increased, the chances of encountering a classical resonance zone have not been increased as compared to the explicitly time-dependent Hamiltonian $H(t)$ in Eq. (3.4) because the two problems are exactly equivalent to each other, differing only by a canonical transformation. It should be noted that the numerical effort involved in integrating the equations of motion in extended phase space has increased.

Tables IV and V are for the same field strengths as Tables I and II but for $m=0$. Most of the trends observed in Tables I and II can also be seen for $m=0$ states. As noted in Sec. II A there are two families of trajectory when $m=0$ depending on the sign of Λ. Trajectories with $\Lambda<0$ [see Figs. 7(a) and 7(b)] lie predominately along either the u or the v axes and are typical of

TABLE V. Energy eigenvalues for $m=0$ states with $\gamma=0.01$ and $\Theta=1.0\times10^{4}$. The paramagnetic energy ($s_z=-\frac{1}{2}$) has been included. Λ is the quantized value of the classical adiabatic invariant, E^{QM} the exact quantum-variational results (Ref. 24), E^{PT} the second-order quantum-perturbation theory (Ref. 16), E^{AS} the adiabatic switching results (average of 25 trajectories), and ΔE^{AS} the standard deviations of the adiabatic switching results.

n	m	r	Λ	E^{QM}	E^{PT}	E^{AS}	ΔE^{AS}
1	0	0	0.000 000 00	0.504 975 0	0.504 975 0	0.504 994	7.0×10^{-11}
2	0	0	−0.250 000 00	0.129 850 0	0.129 850 0	0.129 925	3.0×10^{-8}
2	0	1	1.750 000 00	0.129 652 0	0.129 652 0	0.129 726	6.0×10^{-8}
3	0	0	−0.311 805 39	0.060 047 9	0.060 048 6	0.060 213	3.0×10^{-7}
3	0	1	0.444 444 44	0.059 687 8	0.059 690 9	0.059 841	1.0×10^{-7}
3	0	2	2.534 002 80	0.058 669 3	0.058 677 6	0.058 820	4.0×10^{-7}
4	0	0	−0.353 069 42	0.035 006 3	0.035 030 6	0.035 298	2.3×10^{-6}
4	0	1	−0.020 237 97	0.034 628 7	0.034 668 7	0.034 785	1.0×10^{-5}
4	0	2	1.228 069 40	0.032 917 9	0.033 015 9	0.033 143	4.0×10^{-6}
4	0	3	2.895 237 90	0.030 637 4	0.031 092 1	0.030 836	4.0×10^{-6}

vibrational states with $r \leq 6$ in Table IV. These trajectories are associated with motion in the valleys of the potential energy surface in parabolic coordinates; in cylindrical coordinates the motion is primarily along the z axis. The second type of trajectory, shown in Figs. 7(c) and 7(d), and representative of the rotational states has $\Lambda > 0$ ($r \geq 7$) and these trajectories are directed along axes at 45° to the u and v axes, corresponding to motion along the potential ridge,[59,60,52] i.e., along the ρ axis in cylindrical coordinates. The very-high-lying states (high r) are strongly localized along the potential ridge and their remarkable stability can be understood by parameterizing the problem in one dimension as a Whittaker-Hill equation.[6] It is these states which are quantized in approximate one-dimensional semiclassical treatments[46–51] and which give rise to the strong $1.5\hbar\omega$-spaced quasi-Landau resonances observed in the spectrum close to and above threshold. The transition between the two families of trajectory can be seen by examining typical quantized trajectories for states with $r = 6$ and 7. These trajectories, shown in Figs. 7(b) and 7(c), are both near the separatrix, but on opposite sides of it, and as in Table I a local maximum is observed in the standard deviations of the AS eigenvalues for this pair of states. For completeness the AS results comparable to Table II but for $m = 0$ are compared with exact quantum and quantum perturbation results in Table V. The quantum-perturbation results are generally in slightly better agreement with the exact results than are the AS eigenvalues for these states (note that the energies all

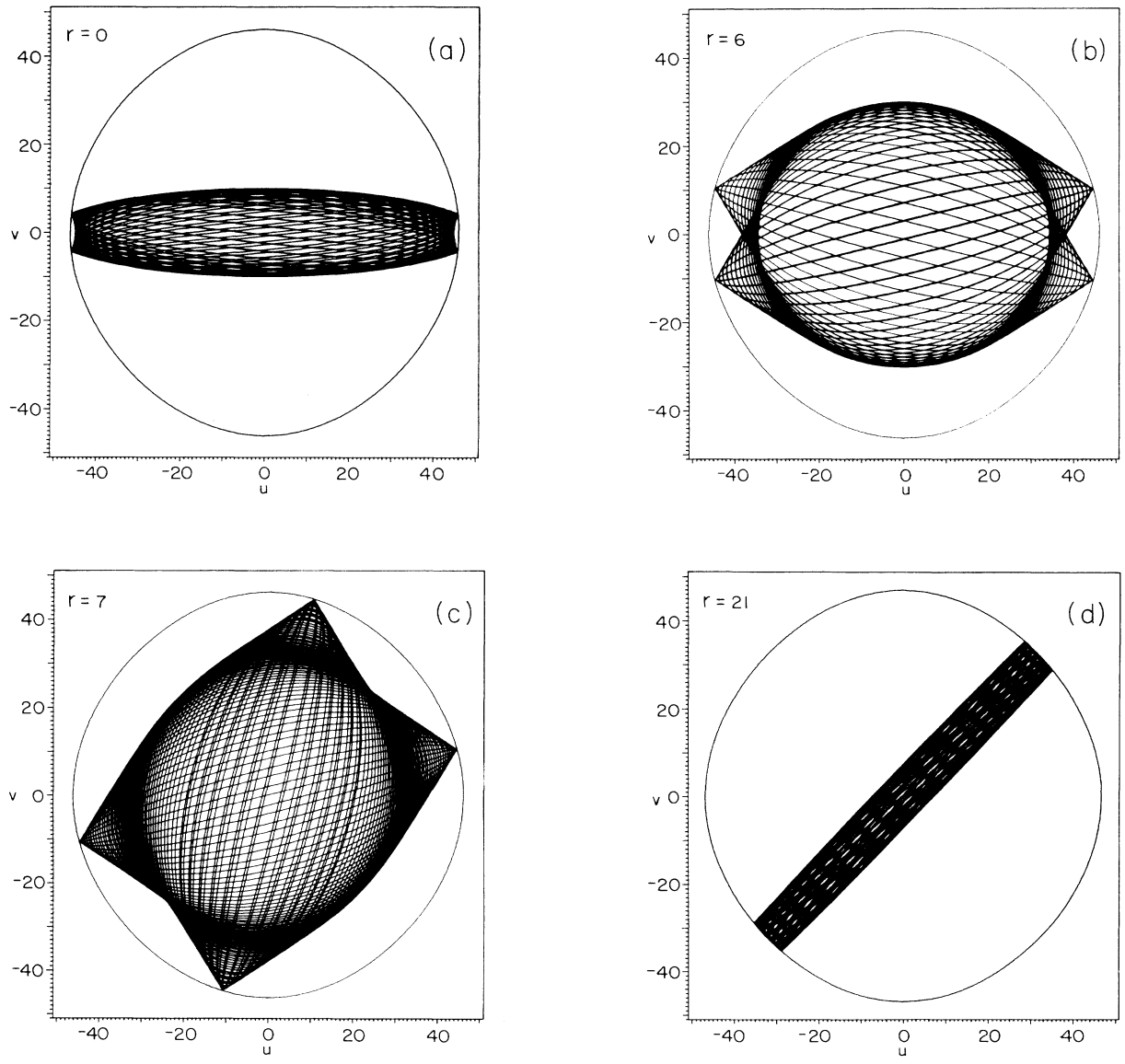

FIG. 7. Representative quantized trajectories obtained using AS for some of the states in Table IV. The trajectories with $r = 6$ and 7 are close to, but on opposite sides of, the separatrix.

correspond to regular classical dynamics—see Fig. 7), but the AS results are still in acceptable agreement with quantum results.

IV. CONCLUSIONS

A comprehensive application of the AS procedure has been made to the problem of a hydrogen atom in a strong magnetic field, i.e., the quadratic Zeeman effect. The QZE, a strongly chaotic system, is an important problem both in atomic physics and in the development of semiclassical quantization procedures for nonseparable, nonintegrable problems. The cases with $m=0$ and $|m|>0$ were treated separately because when $m=0$ the Coulomb singularity makes integration of Hamilton's equations of motion numerically impractical in cylindrical coordinates. The Coulomb singularity was removed using the technique of classical regularization which resulted in a coupled-oscillator-like Hamiltonian for the case $m=0$. A detailed examination of the classical dynamics of the QZE effect was presented for a wide variety of energies and magnetic field strengths for both the case $m=0$ and $|m|>0$. In particular, the topologies of the classical trajectories were related to the sign of the classical adiabatic invariant Λ obtained by Solov'ev using classical perturbation theory. In order to deal with the Coulomb singularity when $m=0$ a new time-independent approach to AS was developed.

Overall, the time-dependent and time-independent AS methods provided excellent agreement with quantum results when the dynamics was regular. Although the AS procedure was extended into mildly chaotic volumes of classical phase space and gave acceptable agreement with quantum results, as the chaos became stronger the method started to fail. In particular, in regions where the quantum levels exhibited multiple avoided crossings the AS procedure was observed to break down. Although in previous applications AS has been applied successfully to model coupled oscillator problems even in chaotic volumes of phase space (e.g., the Henon-Heiles Hamiltonian[91]), these problems generally exhibited weaker chaos than the QZE and, in addition (or, perhaps, consequently[67]), there were far fewer avoided crossings of levels. The semiclassical quantization of the QZE in strongly chaotic volumes of phase space thus remains an open problem.

ACKNOWLEDGEMENTS

It is a pleasure to acknowledge numerous useful conversations on the QZE with W. P. Reinhardt, B. R. Johnson (MIT), A. Deprit, B. Miller, T. P. Grozdanov, and H. S. Taylor. The calculations were performed using the CRAY XMP at the San Diego Supercomputer Center. This work was supported in part by the National Science Foundation through Grant No. CHE-8518873, and by a grant from the Petroleum Research Fund administered by the American Chemical Society.

APPENDIX: QUANTIZATION OF Λ

The zeroth-order problem is taken to be the hydrogen atom, and the quantum-mechanical operator corresponding to Λ is defined using Eqs. (2.4) and (2.5). The problem is to construct a representation $|nrm\rangle$ in which H_0, Λ, and L_z are diagonal. The eigenvalues of Λ can be found either semiclassically or quantum mechanically. Solov'ev[54] proposed a semiclassical quantization scheme which indirectly quantizes the classical quantity Λ. Alternatively, the Schrödinger equation separates in elliptical cylindrical coordinates on the Fock hypersphere, and the eigenvalues may be obtained by solving the resulting associated Lamé equations.[56,104] The most straightforward approach is quantum mechanical and involves constructing the $|nrm\rangle$ representation directly from parabolic basis functions, as described by Grozdanov and Taylor.[16]

Following Grozdanov and Taylor,[16] the parabolic basis functions $|nsm\rangle$ are used where

$$s=0,1,\ldots,k,\quad k=n-|m|-1 \tag{A1}$$

and the relation to the parabolic quantum numbers n_1 and n_2 is given by $n_1=s$ and $n_2=k-s$. In the parabolic basis, A_z is diagonal with eigenvalues $2s-k$.[3] The zeroth-order basis states $|nrm\rangle$ may be expanded in terms of the parabolic basis states,

$$|nrm\rangle=\sum_{s=0}^{k} C_{rs}^{nm}|nsm\rangle\ , \tag{A2}$$

where $r=0,1,\ldots,k$, and because the states are of well-defined parity

$$C_{rk-s}^{nm}=(-1)^{k-r}C_{rs}^{nm}\ . \tag{A3}$$

Using the well-known relations for angular-momentum operators in a parabolic basis,[3] it can be demonstrated that in the $|nsm\rangle$ basis, the only nonzero matrix elements of Λ are the following:

$$\langle nsm|\Lambda|nsm\rangle=2(n^2-m^2-1)-3(2s-k)^2\ , \tag{A4}$$

$$\begin{aligned}\langle n(s+1)m|\Lambda|nsm\rangle&=\langle nsm|\Lambda|n(s+1)m\rangle\\&=4[(k-s)(n-k+s)(n-s-1)(s+1)]^{1/2}\ ,\end{aligned} \tag{A5}$$

and the secular determinant is tridiagonal. The coefficients in the expansion (A2) are given by

$$C_{rs}^{nm}=(-1/4)^s\left[\frac{|m|!(n-s-1)!(k-s)!}{(n-m)!k!s!(|m|+s)!}\right]\times D_{s(\lambda_r)}^{nm}C_{r0}^{nm}\ , \tag{A6}$$

where $D_s(\lambda)$ is a secular determinant, and the eigenvalues of Λ are given as roots of the secular equation

$$D_{k+1}^{nm}(\lambda_r)=0\ , \tag{A7}$$

and for fixed n and m there are $n-|m|$ such eigenvalues of Λ. More details are given in Ref. 16. For $n<4$ Eq. (A7) can be solved analytically. In other cases it is easy to solve the secular equation (A7) using standard routines to obtain quantized values of Λ for any desired state. Once quantized values of H_0 and Λ have been obtained, appropriate initial conditions on the surface of the zeroth-order torus are generated as described in Sec. III A.

*Present address: Theoretical Atomic and Molecular Physics Group, Lawrence Livermore National Laboratory, Livermore, CA 94550.

[1]J. E. Bayfield, Phys. Rep. **51**, 317 (1979) and references therein.

[2]C. Lanczos, Z. Phys. **68**, 204 (1931).

[3]L. D. Landau and E. M. Lifshitz, *Quantum Mechanics* (Pergamon, Oxford, 1977), Secs. 76,77.

[4]D. Farrelly and W. P. Reinhardt, J. Phys. B **16**, 2103 (1983).

[5]*Atomic, Molecular, and Optical Physics,* Vol. 2 of *Physics Through the 1990's* (National Academy Press, Washington, D.C., 1986), p. 63.

[6]J. C. Gay in *Photophysics and Photochemistry in the Vacuum Ultraviolet,* edited by S. P. McGlynn *et al.* (Reidel, Dordrecht, 1985), p. 631.

[7]D. Kleppner, M. G. Littman, and M. L. Zimmerman, in *Rydberg States of Atoms and Molecules,* edited by R. F. Stebbings and F. B. Dunning (Cambridge University Press, Cambridge, 1983).

[8]H. C. Praddaude, Phys. Rev. A **6**, 1321 (1972).

[9]J. E. Avron, B. G. Adams, J. Cizek, M. Clay, M. L. Glasser, P. Otto, J. Paldus, and E. Vrscay, Phys. Rev. Lett. **43**, 691 (1979).

[10]J. E. Avron, Ann. Phys. (N.Y.) **131**, 73 (1981).

[11]H. J. Silverstone and R. K. Moats, Phys. Rev. A **23**, 1645 (1981).

[12]A. V. Turbiner, Z. Phys. A **308**, 111 (1982).

[13]J. N. Silverman, Phys. Rev. A **28**, 498 (1983).

[14]E. A. Solov'ev, Zh. Eksp. Teor. Fiz. **85**, 109 (1983) [Sov. Phys.—JETP **58**, 63 (1983)].

[15]A. C. Chen, Phys. Rev. A **29**, 2225 (1984).

[16]T. P. Grozdanov and H. S. Taylor (unpublished).

[17]C. Angelié and C. Deutsch, Phys. Lett. A **67**, 357 (1978).

[18]W. P. Reinhardt and D. Farrelly, J. Phys. (Paris) Colloq. **43**, C2-2 (1982).

[19]Y. Yafet, R. W. Keyes, and E. W. Adams, J. Phys. Chem. Solids **1**, 137 (1956).

[20]M. L. Zimmerman, M. M. Kash, and D. Kleppner, Phys. Rev. Lett. **45**, 1092 (1980).

[21]C. W. Clark and K. T. Taylor, J. Phys. B **13**, L737 (1980).

[22]C. W. Clark and K. T. Taylor, J. Phys. B **15** 1175 (1982).

[23]C. W. Clark and K. T. Taylor, Comp. Phys. Commun. **26**, 415 (1982).

[24]W. Rosner, G. Wunner, H. Herold, and H. Ruder, J. Phys. B **17**, 29 (1984).

[25]G. Wunner, J. Phys. B **19**, 1623 (1986).

[26]D. Wintgen and H. Friedrich, J. Phys. B **19**, 1261 (1986).

[27]D. Wintgen and H. Friedrich, J. Phys. B **19**, 991 (1986).

[28]D. Wintgen and H. Friedrich, J. Phys. B **19**, L99 (1986).

[29]D. Wintgen and H. Friedrich, Phys. Rev. Lett. **57**, 571 (1986).

[30]D. Delande, F. Biraben, and J. C. Gay, *New Trends in Atomic Physics,* Les Houches Lectures, Session XXXVIII (Elsevier, Amsterdam, 1984) p. 351.

[31]J. R. P. Angel, Astrophys. J. **216**, 1 (1977).

[32]J. R. P. Angel, Ann. Rev. Astron. Astrophys. **16**, 487 (1978).

[33]J. C. Kemp, J. B. Swedlund, J. D. Landstreet, and J. R. P. Angel, Astrophys. J. Lett. **189**, L79 (1980).

[34]M. Robnik, J. Phys. A **14**, 3195 (1981)

[35]A. K. Ramdas and S. Rodriguez, Rep. Prog. Phys. **44**, 1297 (1981)

[36]R. H. Garstang, Rep. Prog. Phys. **40**, 105 (1977).

[37]J. P. Connerade, J. C. Gay, and S. Liberman, Comments At. Mol. Phys. **13**, 189 (1983).

[38]C. W. Clark, K. T. Lu, and A. F. Starace, in *Progress in Atomic Spectroscopy, Part C,* edited by H. J. Berger and H. Kleinpoppen (Plenum, New York, 1984), p. 247.

[39]J. C. Gay, in *Progress in Atomic Spectroscopy, Part C,* edited by H. J. Berger and H. Kleinpoppen (Plenum, New York, 1984), p. 177.

[40]J. Phys. (Paris) Colloq. C2, **43** (1982), entire issue.

[41]W. R. S. Garton and F. S. Tomkins, Astrophys. J. **158** 839 (1969).

[42]K. T. Lu, F. S. Tomkins, H. M. Crosswhite, and H. Crosswhite, Phys. Rev. Lett. **41**, 1034 (1978).

[43]K. T. Lu, F. S. Tomkins, and W. R. S. Garton, Proc. R. Soc. London, Ser. A **364**, 421 (1978).

[44]A. Holle, G. Wiebusch, J. Main, B. Hager, H. Rottke, and K. H. Welge, Phys. Rev. Lett. **56**, 2594 (1986).

[45]D. Delande, C. Chardonnet, F. Biraben, and J. C. Gay, J. Phys. (Paris) Colloq. **43**, C2-97 (1982).

[46]A. R. Edmonds, J. Phys. (Paris) Colloq. **31**, C4-71 (1970).

[47]A. F. Starace, J. Phys. B **6**, 585 (1973).

[48]R. F. O'Connell, Astrophys. J **187**, 275 (1974).

[49]A. R. P. Rau, Phys. Rev. A **16**, 613 (1977).

[50]A. R. P. Rau, Bull. Am. Phys. Soc. **23**, 10 (1978).

[51]A. R. P. Rau, J. Phys. B **12**, L193 (1979).

[52]C. W. Clark and K. T. Taylor, Nature **292**, 437 (1981).

[53]E. A. Solov'ev, Pis'ma Zh. Eskp. Teor. Fiz. **61**, 500 (1971) [JETP Lett. **34**, 265 (1981)].

[54]E. A. Solov'ev, Zh. Eskp. Teor. Fiz. **82**, 1762 (1982) [Sov. Phys.—JETP **55**, 1017 (1982)].

[55]C. W. Clark, Phys. Rev. A **24**, 605 (1981).

[56]D. R. Herrick, Phys. Rev. A **26**, 323 (1982).

[57]D. Delande and J. C. Gay, J. Phys. B **17**, L335 (1984).

[58]J. C. Gay, D. Delande, F. Biraben, and F. Penet, J. Phys. B **16**, L693 (1983).

[59]U. Fano, Colloq. Int. CNRS **273**, 127 (1977).

[60]U. Fano, J. Phys. B **13**, L519 (1980).

[61]A. R. Edmonds and R. A. Pullen (unpublished).

[62]J. B. Delos, S. K. Knudson, and D. W. Noid, Phys. Rev. A. **28**, 7 (1983); **30**, 1208 (1984).

[63]J. B. Delos, S. K. Knudson, and D. W. Noid, Phys. Rev. Lett. **50** 579 (1983).

[64]D. W. Noid, S. K. Knudson, and J. B. Delos, Chem. Phys. Lett. **100**, 367 (1983).

[65]D. Richards, J. Phys. B **16**, 749 (1983).

[66]M. A. Al-Laithy, C. M. Farmer, and M. R. C. McDowell, Phys. Lett. **108A**, 144 (1985).

[67]D. W. Noid, M. L. Koszykowski, and R. A. Marcus, Annu. Rev. Phys. Chem. **32**, 267 (1981).

[68]D. W. Noid and R. A. Marcus J. Chem. Phys. **62**, 2119 (1975).

[69]W. P. Reinhardt, in *Chaotic Behavior in Quantum Systems: Theory and Applications,* edited by G. Casati (Plenum, New York, 1985), p. 235.

[70]W. P. Reinhardt, in *The Mathematical Analysis of Physical Systems,* edited by R. Mickens (Van Nostrand Reinhold, New York, 1985), p. 169.

[71]E. J. Heller and E. B. Stechel, Ann. Rev. Phys. Chem. **33**, 563 (1984).

[72]T. Uzer and R. A. Marcus, J. Chem. Phys. **81**, 5013 (1984).

[73]T. Uzer, Chem. Phys. Lett. **110**, 356 (1984).

[74]D. Farrelly, J. Chem. Phys. **85**, 2119 (1986).

[75]J. A. C. Gallas, G. Leuchs, H. Walther, and H. Figger, Adv. Atom. Mol. Phys. **20**, 413 (1985).

[76]M. L. Zimmerman, J. C. Castro, and D. Kleppner, Phys. Rev. Lett. **40**, 1083 (1978).

[77]J. C. Castro, M. L. Zimmerman, R. G. Hulet, and D. Kleppner, Phys. Rev. Lett. **45**, 1780 (1980).
[78]J. C. Gay, D. Delande, and F. Biraben, J. Phys. B **13**, L729 (1980).
[79]D. Delande and J. C. Gay, Phys. Lett. **82A**, 399 (1981).
[80]P. Cacciani, E. Luc-Koenig, J. Pinard, C. Thomas, and S. Liberman, Phys. Rev. Lett. **56**, 1124 (1986).
[81]P. Cacciani, E. Luc-Koenig, J. Pinard, C. Thomas, and S. Liberman, J. Phys. B **19**, L519 (1986).
[82]M. Robnik and E. Schrüfer, J. Phys. A. **18**, L853 (1985).
[83]D. Delande and J. C. Gay, Phys. Rev. Lett. **57**, 2006 (1986).
[84]D. Delande, A. Steitz, and J. C. Gay, in *Oji International Seminar on Highly Excited States of Atoms and Molecules,* edited by S. S. Kano and M. Matsuzamo (Fuji-Yoshida, Japan, 1986), p. 61.
[85]R. B. Shirts and W. P. Reinhardt, J. Chem. Phys. **77**, 5204 (1982).
[86]S. L. Coffey, A. Deprit, B. Miller, and C. A. Williams, in *Chaotic Pheonomena in Astronomy,* Proceedings of the Second Florida Workshop on Nonlinear Astronomy [Ann. N.Y. Acad. Sci. (to be published)].
[87]E. A. Solov'ev, Zh. Eksp. Teor. Fiz. **75**, 1261 (1978) [Sov. Phys.—JETP **48**, 635 (1978)].
[88]T. P. Grozdanov and E. A. Solov'ev, J. Phys. B **15**, 1195 (1982).
[89]B. R. Johnson (unpublished).
[90]B. R. Johnson, J. Chem. Phys. **83**, 1204 (1985); **86**, 1445 (1987).
[91]R. T. Skodje, F. Borondo, and W. P. Reinhardt, J. Chem. Phys. **82**, 4611 (1985).
[92]R. M. Hedges, R. T. Skodje, F. Borondo, and W. P. Reinhardt, Am. Chem. Soc. Symp. Ser. No. **263**, 323 (1984).
[93]T. P. Grozdanov, S. Saini, and H. S. Taylor, Phys. Rev. A **33**, 55 (1986).
[94]T. P. Grozdanov, S. Saini, and H. S. Taylor, J. Chem. Phys. **84**, 3243 (1986).
[95]J. W. Zwanziger, E. R. Grant, and G. S. Ezra, J. Chem. Phys. **85**, 2089 (1986).
[96]A. Barthelemy and J. Arnaud, J. Opt. Soc. Am. **71**, 32 (1981).
[97]C. Jaffé, J. Chem. Phys. **85**, 2885 (1986).
[98]M. Kruskal, J. Math. Phys. **3**, 806 (1962).
[99]M. V. Berry, J. Phys. A **17**, 1225 (1984).
[100]G. Casati, B. V. Chirikov, I. Guarneri, and D. L. Shepelyansky, Phys. Rev. Lett. **56**, 2437 (1986).
[101]A. J. Lichtenberg and M. A. Lieberman, *Regular and Stochastic Motion* (Springer-Verlag, New York, 1983).
[102]H. Hasegawa, A. Harada, and Y. Okazaki, J. Phys. A **17**, L883 (1984).
[103]E. G. Kalnins, W. Miller, and P. Winternitz, SIAM J. Appl. Math. **30**, 630 (1970).
[104]J. W. B. Hughes, Proc. Phys. Soc. **91**, 810 (1967).
[105]D. Farrelly and T. Uzer, J. Chem. Phys. **85**, 308 (1986).
[106]V. G. Szebehely, *Theory of Orbits* (Academic, New York, 1967).
[107]V. A. Dulock and H. V. McIntosh, Pac. J. Math. **19**, 39 (1966).
[108]P. Kustaanheimo and E. Steifel, J. Reine Angew. Math. **218**, 204 (1965).
[109]A. C. Chen, Phys. Rev. A **22**, 333 (1980).
[110]A. C. Chen and M. Kibler, Phys. Rev. A **31**, 3960 (1985).
[111]P. Ehrenfest, in *Sources of Quantum Mechanics,* edited by B. L. van Der Waerden (Dover, New York, 1967), an abridged translation of the original article in Versl. Kon. Akad. Amsterdam **25**, 412 (1916).
[112]G. Baym, *Lectures in Quantum Mechanics* (Benjamin Cummings, Menlo Park, 1973), Chap. 7.
[113]G. Hose, H. S. Taylor, and D. Richards, J. Phys. B **18**, 51 (1985).